Hydrogen vibrational modes and anisotropic potential in α-ScH_x

T. J. Udovic and J. J. Rush
Materials Science and Engineering Laboratory, National Institute of Standards and Technology, Gaithersburg, Maryland 20899

I. S. Anderson
Paul Scherrer Institut, CH-5232 Villigen PSI, Switzerland

R. G. Barnes
Ames Laboratory and Department of Physics, Iowa State University, Ames, Iowa 50011
(Received 28 September 1989)

The hydrogen vibrational spectra of single-crystal α-ScH_x ($x=0.05$, 0.16, and 0.25) have been measured using incoherent-inelastic-neutron-scattering methods. Alignment of the momentum-transfer vector Q either perpendicular or parallel to the c axis permitted the selective enhancement in scattering sensitivity of the different normal modes of the tetrahedrally bound hydrogen. The results show that the c-axis vibration peak (at ca. 103 meV) is over 30% lower in energy than the doubly degenerate basal-plane modes (at ca. 148 meV) and possesses considerable anharmonicity, as reflected by the ratio (1.76) of the second- to first-excited-state energies. High-resolution neutron spectra for the c-axis vibrations revealed a peak at all hydrogen concentrations that is much broader (ca. 14 meV full width at half maximum intrinsic linewidth, $x=0.25$) than the instrumental resolution, yet devoid of any resolved fine structure indicative of a distinct local-mode splitting as was observed previously for α-YH_x. This suggests that although local ordering via hydrogen pairing across a Sc atom exists within α-ScH_x at low temperature, ordering of the hydrogen pairs themselves along the c axis is less extensive than in α-YH_x.

INTRODUCTION

In recent years, numerous studies have been undertaken to characterize the structure and dynamics of hydrogen in several of the rare-earth hcp metals (namely, Lu, Y, and Sc) that form "α-phase" solid solutions with hydrogen. These solutions can possess relatively high H concentrations[1] [e.g., $x_{max}\approx 0.35$ for α-ScH_x (Ref. 2)] and are stable even at low temperatures approaching absolute zero.[3] The H atoms are known to reside in the tetrahedral interstices (i.e., t sites) of the metal host lattice.[4-7] A typical characteristic of these systems is a concentration-independent electrical resistivity anomaly occurring between 150 and 170 K which was originally attributed to the onset of short-range ordering of H atoms into pairs.[3] Subsequent results of diffuse elastic neutron scattering (DENS) studies of α-LuD_x (Refs. 8 and 9) and α-YD_x (Refs. 10 and 11) indicate that in the α phase, D (H) atoms, indeed, have a tendency to pair along the c axis at second-neighbor distances with the D (H) atoms in each pair separated by a metal atom. Yet, the DENS results also suggest that the resistivity anomaly is due to long-range ordering of the H pairs rather than to the formation of the pairs themselves. For α-$YD_{0.17}$,[10,11] the data were consistent with a model invoking the one-dimensional intraline ordering of existing pairs along the c axis upon cooling through the anomaly temperature, with little or no correlation between lines. For α-LuD_x ($x=0.04$ and 0.19), the data were consistent with a similar model invoking the intraline ordering of pairs along the c axis, but with interline correlations also present. In addition, a recent reference to to-be-published neutron scattering results for α-ScH_x (Ref. 12) indicates that a similar intraline ordering of H pairs along the c axis was found in this system. NMR measurements[13] of the proton (^{1}H) spin-lattice relaxation rate in α-ScH_x are also consistent with the existence of H pairs, but suggest little long-range order, resulting in a "proton glass" state within the Sc lattice.

In addition to the above-mentioned studies, incoherent-inelastic neutron-scattering (IINS) experiments have been carried out to characterize the hydrogen-bonding potentials that exist for the t sites in the rare-earth metals. In a previous investigation, high-resolution IINS measurements[14] of the hydrogen local-mode frequencies in single-crystal samples of α-YH $(D)_{0.18}$ demonstrated a highly anisotropic potential which was much softer and anharmonic along the c axis than in the basal plane. Despite nearly cubic first-neighbor symmetry for the t sites (i.e., a c/a ratio that is only 3% less than the ideal value), the vibrational mode along the c axis exhibited an energy that was 25% lower than that of the doubly degenerate vibrations in the basal plane. Moreover, the c-axis mode possessed a novel splitting which was attributed to the existence of H pairs dynamically coupled across metal atoms along the c axis (as suggested by the DENS results[9]). The variation in vibrational line shape of this split feature with H concentration and temperature found in subsequent IINS measurements[15] suggested that the H-H pair interaction is

modulated by concentration- and temperature-dependent occupation correlations along the c axis.

Somewhat lower-resolution IINS measurements of the deuterium local-mode energies in α-$LuD_{0.19}$ (Ref. 16) and α-ScD_x ($x=0.19$ and 0.33) (Ref. 12) have also indicated the existence of a vibrational anistropy with the energy of the c-axis mode 30% lower than that of the basal plane modes. An apparent splitting of the c-axis mode was reported for α-$LuD_{0.19}$, again suggestive of H pairing. The measurements on α-ScD_x were performed with a resolution of ca. 6 meV and showed no observable splitting of the c-axis mode, leading the authors to conclude that a direct D-D interaction is much smaller or absent in α-ScD_x (compared to α-$LuD_{0.19}$) and is not essential for pair formation.

In the present investigation, we have performed both low- and high-resolution IINS measurements on α-ScH_x in order to characterize the hydrogen-bonding potential at the t sites and to compare these results with the earlier results on the yttrium-hydrogen system. In particular, hydrogen vibrational spectra of α-ScH_x ($x=0.05$, 0.16, and 0.25) were collected to investigate the magnitude of anisotropy in the hydrogen-bonding potential and to probe the extent and nature of H pairing along the c-axis via line-shape analysis of the c-axis local mode.

EXPERIMENTAL DETAILS

Three single-crystal disks of scandium were supplied by the Ames Laboratory Materials Preparation Center at Iowa State University. Each disk was approximately 10 g, 40-mm diameter×3 mm thick, and cut from the same ingot with the c axis oriented perpendicular to the crystal face. The thin-plate geometry of the crystal was necessitated by the significant neutron absorption cross section for Sc. One crystal was used as a blank, one was loaded with hydrogen to a composition of α-$ScH_{0.05}$, and one was loaded with hydrogen at different stages of the investigation to two different compositions, α-$ScH_{0.16}$ and α-$ScH_{0.25}$. The hydrogen loading was accomplished in the normal fashion by gas-phase absorption using a calibrated dose volume to titrate the desired concentrations. After loading at 700 K, the crystals were annealed for 12 h at 800 K, cooled to room temperature, and mounted into a variable-temperature cryostat or displex for spectral analysis.

The IINS measurements were performed at the Neutron Beam Split-Core Reactor (NBSR) at the National Institute of Standards and Technology using the BT-4 triple-axis spectrometer. Incident energies were selected using a Cu(220) monochromator. Broad spectral scans were taken in a low-resolution configuration consisting of 40′ collimators before and after the monochromator and a liquid-nitrogen-cooled Be filter before the neutron detector. In this configuration, the instrumental resolution varied between 5 and 16 meV full width at half maximum (FWHM) over the scan range from 50 to 230 meV. Whenever possible, spectral peaks were fitted with Gaussian line shapes in order to determine their positions and widths. More detailed investigations of vibrational line shapes were accomplished in the high-resolution configuration consisting of 20′ collimators before and after the monochromator and a liquid-nitrogen-cooled Be-graphite-Be composite filter before the neutron detector. In this configuration, the instrumental resolution was 2.5 meV at 100 meV energy transfer.

As done in the IINS study of $YH_{0.18}$,[14] it was possible to orient the crystal and neutron detector so as to align the momentum transfer vector $\mathbf{Q}$ at an approximately constant angle of choice (e.g., either perpendicular or parallel) to the c axis of the crystal. By varying this angle appropriately, one could attain the selective enhancement in neutron scattering intensity for the different hydrogen normal-mode vibrations. In the limit of one-quantum scattering, the neutron scattering intensity is proportional to, among other things, the squared dot product $(\mathbf{Q}\cdot\mathbf{C}_j)^2$ where $\mathbf{C}_j$ is the hydrogen displacement vector for the jth normal mode.[17] Thus, scattering intensity is maximized for those normal-mode vibrations polarized in the direction of $\mathbf{Q}$ and decreases toward zero for those normal-mode vibrations polarized in a direction perpendicular to $\mathbf{Q}$.

RESULTS

Figure 1 shows the low-resolution vibrational spectra of α-$ScH_{0.16}$ as a function of the angle ψ between $\mathbf{Q}$ and the c axis. For $\mathbf{Q}$ perpendicular to the c axis [$\psi=90°$, Fig.

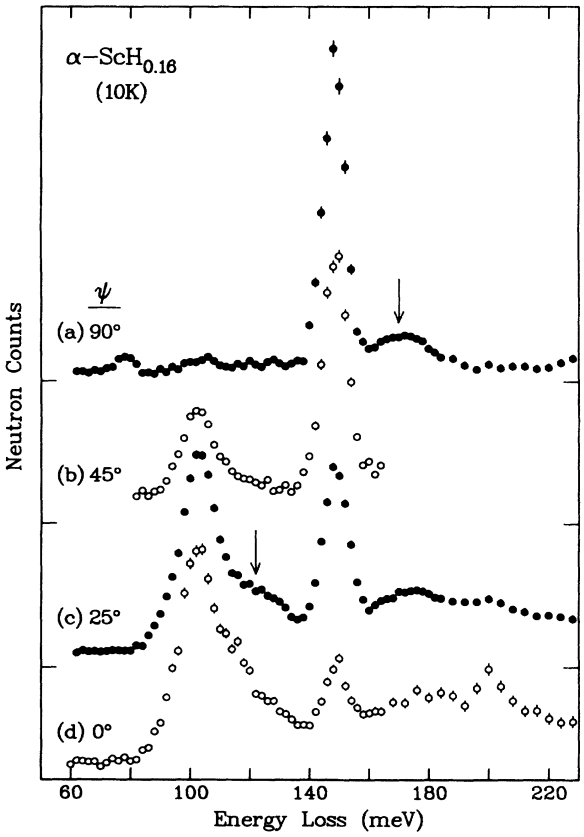

FIG. 1. Low-resolution IINS spectra of α-$ScH_{0.16}$ at 10 K as a function of ψ, the angle between $\mathbf{Q}$ and the c axis. Positions of multiphonon scattering sidebands are marked with arrows.

1(a)], the scattering intensity of the c-axis mode is necessarily zero (i.e., $\mathbf{Q}\cdot\mathbf{C}_c=0$), whereas the scattering intensity of the doubly degenerate basal-plane modes is maximized (i.e., $\mathbf{Q}\cdot\mathbf{C}_{ab}=QC_{ab}$) as indicated by the single dominant scattering feature at 148.3 meV. As Q approaches the direction of the c axis [$\psi\rightarrow 0°$, Figs. 1(b)–1(d)], both types of modes are now observable. The emergence and growth of a scattering feature at 102.8 meV concomitant with the attenuation of the basal-plane mode as ψ approaches 0° identifies this feature as due to the c-axis mode. Failure of the basal-plane feature at 148.3 meV to completely disappear in Fig. 1(d) indicates that the c axis of the crystal was not perfectly aligned in the Q direction, thus allowing some scattering from modes of the wrong polarization.

In addition to the main scattering peaks, weak features at 78 meV in Fig. 1(a) and at 200 meV in Figs. 1(c) and 1(d) are artifacts due to incompletely filtered Bragg scattering of the incident beam from the single-crystal sample into the neutron detector. These weak features could be made to disappear with the appropriate repositioning of the neutron detector (i.e., by varying the angle between the incident beam and the scattered beam).

The spectra in Fig. 1 also display sidebands centered at ca. 122 and 170 meV, roughly 20 meV above the main vibrational features. Analogous sidebands have also been observed for the α-YH_x system.[18] Subsequent IINS spectra of α-$ScH_{0.25}$ as a function of temperature (Figs. 2 and 3) confirm that these sidebands are due to multiphoton scattering processes involving the low-energy motions of hydrogen coupled to the Sc-lattice modes. This follows from the fact that, at 10 K, the population of lattice vibrational levels above the ground state is minimal.

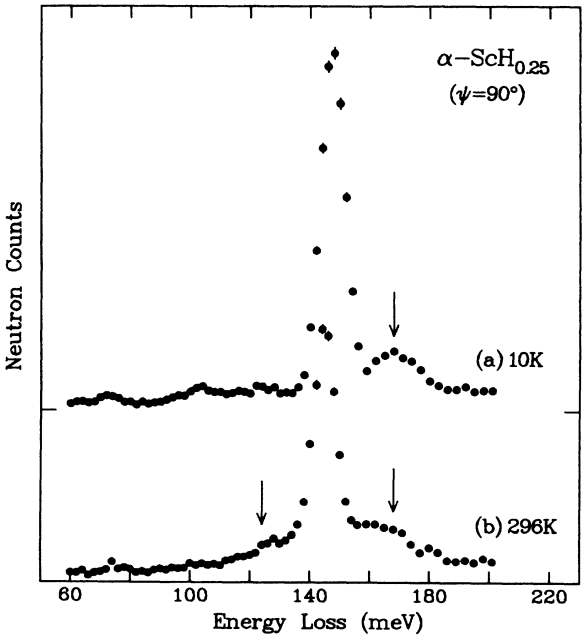

FIG. 2. Low-resolution IINS spectra of α-$ScH_{0.25}$ for $\psi=90°$ (i.e., Q perpendicular to the c axis) as a function of temperature. Positions of multiphonon scattering sidebands are marked with arrows.

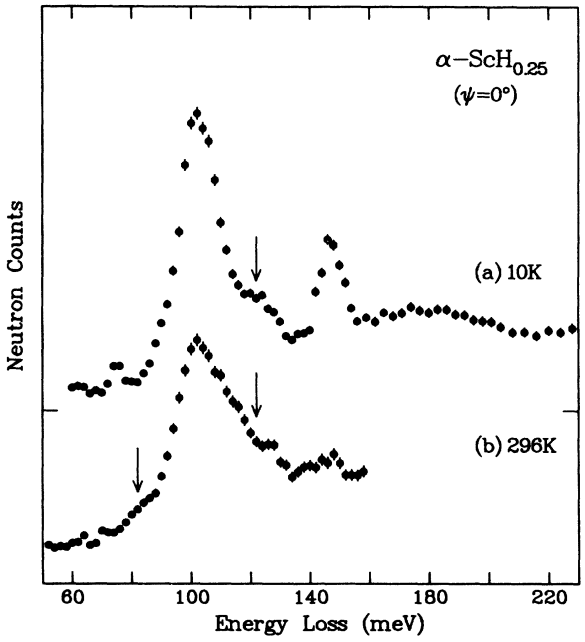

FIG. 3. Low-resolution IINS spectra of α-$ScH_{0.25}$ for $\psi=0°$ (i.e., Q parallel to the c-axis) as a function of temperature. Positions of multiphonon scattering sidebands are marked with arrows.

Hence, multiphonon scattering will only involve neutron energy-loss processes, yielding additional scattering intensity only above the one-phonon peak energy. By contrast, at 296 K, the population of lattice vibrational levels 20 meV (and higher) above the ground state will be appreciable. In this instance, multiphonon scattering will involve both neutron energy-loss and energy-gain processes, yielding additional scattering intensity both above and below the one-phonon peak energy. Indeed, the spectrum of α-$ScH_{0.25}$ [Fig. 2(a)] for Q perpendicular to the c axis at 10 K is similar to that of α-$ScH_{0.16}$ [Fig. 1(a)], indicating the basal-plane vibrational energy at 147.5 meV with only a high-energy sideband centered at ca. 168 meV. Upon warming the crystal to 296 K [Fig. 2(b)], the high-energy sideband smears out and a broad low-energy sideband centered at ca. 124 meV appears, equidistant from the main peak (which has shifted down to 145 meV). Identical behavior occurs for the c-axis mode of α-$ScH_{0.25}$ with Q parallel to the c axis in Fig. 3. At 10 K [Fig. 3(a)], the spectrum shows a c-axis vibrational peak at 102.5 meV with a high-energy sideband centered at ca. 122 meV. [As in Fig. 1(d), the small scattering contribution from the basal-plane modes at ca. 147.5 meV in Fig. 3(a) is a result of an imperfect alignment of Q and the c axis before collecting the spectrum.] At 296 K [Fig. 3(b)], again the high-energy sideband smears out and a broad low-energy sideband centered at ca. 82 meV appears, equidistant from the peak. The observed positions of the multiphonon satellite structure were consistent with measurements of the low-energy phonon distribution for hydrogen in α-$ScH_{0.25}$ using the time-of-flight (TOF) spectrometer at NBSR as well as the phonon-dispersion-curve data reported for Sc metal[19] and α-ScH_x.[12]

It is useful to estimate the degree of anharmonicity in the t-site potential by determining the ratio of the second- to first-excited-state energies ($E_{0\to2}/E_{0\to1}$) for the normal modes. This could not be attempted for the basal-plane modes since the second-excited-state energy is expected at ca. 290–300 meV, which is beyond the spectral range of the instrument. Nonetheless, Figs. 1(d) and 3(a) illustrate vibrational spectra covering the high-energy region with the appropriate Q polarization for observing the second-excited state of the c-axis mode without any significant overlapping multiphonon contributions around 170 meV associated with basal-plane modes. As mentioned previously, Fig. 1(d) possesses a Bragg-scattering artifact centered at 200 meV which interferes with the accurate determination of $E_{0\to2}$. In contrast, Fig. 3(a), free of this artifact, displays a definite broad feature assigned to the second-excited-state energy centered at ca. 180 meV. Despite interference from the 200-meV artifact, Fig. 1(d) also corroborates the presence of this feature. Hence, the estimated ratio of $E_{0\to2}/E_{0\to1}\approx1.76$ demonstrates that a considerable degree of anharmonicity exists for the potential along the c-axis direction, similar to that observed previously for $YH_{0.18}$ ($YD_{0.18}$).[14,18]

Besides the difference in vibrational energies, a careful inspection of the low-temperature spectra in Figs. 1–3 also reveals a significant difference (after resolution corrections) in the peak widths of the c-axis and basal-plane modes for both H concentrations. Gaussian fits of these mode peaks for α-$ScH_{0.25}$ (α-$ScH_{0.16}$) indicate peak widths (FWHM) of 16.0 (15.0) and 9.4 (9.0) meV, respectively. These fits included corrections for overlapping multiphonon scattering sidebands by including additional fitted Gaussian components. Since the respective spectrometer resolutions are 6.9 and 9.0 meV, this implies that the basal-plane mode is almost resolution limited, whereas the c-axis mode has an intrinsic linewidth of ca. 14.4 (13.3) meV. These results are consistent with those found for $YH_{0.18}$,[14,15] and suggested that the c-axis mode possessed a similar splitting due to dynamically coupled H pairs along the c-axis direction.

In view of this, the line shape of the c-axis vibrational peak for α-ScH_x was investigated more closely under high-resolution conditions. In Fig. 4, high-resolution IINS spectra at low temperature for ScH_x are plotted as a function of the H concentration [$x=0.05$ (at 4 K), 0.16 (9 K), and 0.25 (4 K)]. Peak positions and widths were determined by assuming a flat background and fitting only the low-energy portion of the spectra below 106 meV. This is because the high-energy side of the peak is contaminated by multiphonon scattering of uncertain magnitude, which was successfully compensated for in fits of the low-resolution spectra by the addition of another Gaussian component. Both α-$ScH_{0.25}$ and α-$ScH_{0.05}$ spectra were fitted with Gaussian line shapes, whereas the α-$ScH_{0.16}$ spectrum was more successfully fit with a Lorentzian line shape. Because of the limited energy range scanned (i.e., ca 80–140 meV; see Figs. 1 and 3), the exact structure and slope of the spectral wings were not determined. Hence, the differences in fitted line shapes were solely used to determine peak positions and widths, and are not meant to imply any real concentration-dependent differences in the shape of the H density of states.

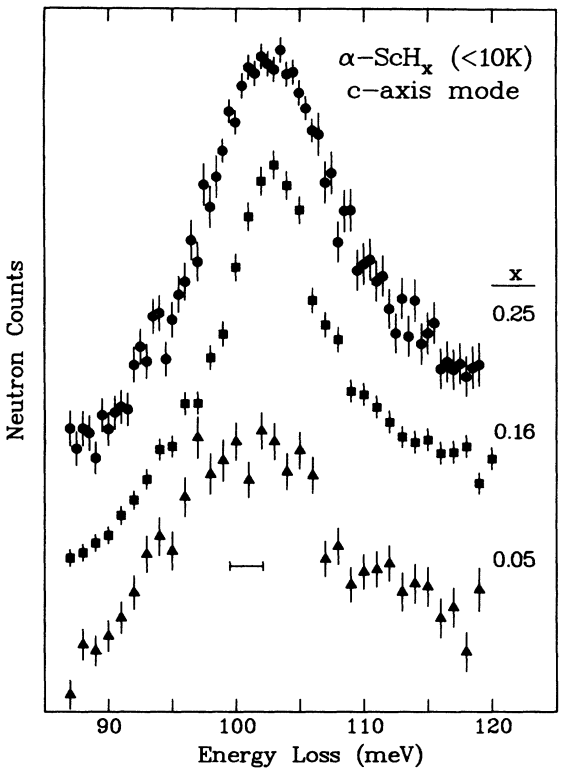

FIG. 4. High-resolution IINS spectra of the c-axis mode at $T<10$ K for α-ScH_x (with $\psi=25°$) as a function of H concentration. The instrumental resolution (FWHM) is illustrated by the horizontal bar beneath the spectra.

The spectra indicate, first, that the peak position shifts from ca. 102.9 meV at the higher H concentrations, $x=0.25$ and 0.16, to ca. 101 meV at the lowest H concentration $x=0.05$. Second, the peak width (FWHM) decreases from 13.0 meV for $x=0.25$ to 12.4 meV for $x=0.16$, which corresponds to intrinsic linewidths of 12.8 and 12.1 meV, respectively. (The poorer spectral statistics for α-$ScH_{0.05}$ did not warrant a meaningful determination of its peak width for comparison.) These are ca. 10% lower than the linewidths determined from the low-resolution results. This discrepancy is to be expected since, as mentioned above, the high-resolution spectra were not collected over a sufficiently broad energy range to completely establish the entire peak shape, as well as the position and slope of the spectral baseline. As a result, the flat baselines chosen for fitting purposes are probably too high, leading to an underestimation of the peak widths. It is clear from the high-resolution spectra that, despite the broad nature of the c-axis mode at all H concentrations, no distinct splitting is visible within the 2.5-meV resolution of the instrument.

DISCUSSION

The results presented in the previous section reveal some interesting similarities and differences between the α-phase solutions of hydrogen in Sc and Y, which are summarized in Table I.

TABLE I. Comparison of single-crystal data for α-ScH_x and α-$YH_{0.18}$ below 10 K. The entries in square brackets refer to data taken under the high-resolution configuration. Note: all errors (in parentheses) are Gaussian fitting errors only, except for Lorentzian fitting errors for the high-resolution α-$ScH_{0.16}$ data and are the errors ($\pm$) in the last digit given.

	Normal-mode energies			c-axis mode			
	(c-axis) E_c (meV)	(Basal-plane) E_{ab} (meV)	E_c/E_{ab}	$E_{0\to2}$	$E_{0\to2}/E_{0\to1}$	Intrinsic FWHM (meV)	Resolved splitting?
α-$YH_{0.18}$ (Refs. 14 and 15)	100.1(2)	134.2(5)	0.746(4)	180(2)[a]	1.80(2)[a] 1.82(1)[b]	9.5	[yes]
α-$ScH_{0.25}$	102.5(2) [102.8(1)]	147.5(1)	0.695(2)	180(2)	1.76(2)	14.4(5) [12.8(7)]	[no]
α-$ScH_{0.16}$	102.8(2) [103.0(1)]	148.3(1)	0.693(2)	180(3)	1.75(3)	13.3(5) [12.1(7)]	[no]
α-$ScH_{0.05}$	[101.0(3)]						[no]

[a]Unpublished result determined from Ref. 18.
[b]Determined from α-$YD_{0.18}$ data.

First, both systems exhibit a highly anisotropic t-site potential which is much softer along the c axis than in the basal plane. The anisotropy is more pronounced for α-ScH_x with a c-axis mode energy over 30% lower than that of the basal-plane modes compared to a 25% softer c-axis mode for α-$YH_{0.18}$.

Second, the observed downward shift of the α-ScH_x c-axis mode from ca. 102.9 meV at $x \geq 0.16$ to 101 meV at $x = 0.05$ is similar to the hydrogen-concentration dependence of the c-axis mode for α-YH_x,[15] which has been attributed to the relaxation of coherent strain ordering as the hydrogen concentration decreases, resulting in a larger average metal-hydrogen separation as more alternative hydrogen configurations become accessible. This effect is partially counteracted by a decrease in the α-ScH_x lattice constants as the hydrogen concentration decreases, which favors a decreasing average metal-hydrogen separation corresponding to increasing normal-mode energies. The c-axis-mode peak positions determined from both low- and high-resolution spectra actually suggest a slight 0.2–0.3 meV increase (albeit at the verge of being within experimental uncertainty) as the hydrogen concentration decreases from $x = 0.25$ to 0.16, before decreasing at lower hydrogen concentration. This lattice-size effect is most evident for the basal-plane modes which shift upward from 147.5 to 148.3 meV as the hydrogen concentration decreases from $x = 0.25$ to 0.16.

Third, the potentials in both systems exhibit considerable anharmonicity in the c direction as illustrated by the ratios of the second- to first-excited-state energies. Again, this anharmonicity is more pronounced for α-ScH_x, which possesses a lower ratio of 1.76 compared to values of 1.80 (1.82) for α-$YH_{0.18}$ (α-$YD_{0.18}$) and 2.0 for the harmonic case.

Lastly, despite the broader apparent linewidth for α-$ScH_{0.25}$ compared to α-$YH_{0.18}$, no resolvable splitting is observed for α-$ScH_{0.25}$ (or lower hydrogen concentrations), whereas a definite 4-meV splitting is observed for α-$YH_{0.18}$. This result is illustrated in Fig. 5 by a comparison of the high-resolution IINS spectra of the c-axis modes at low temperature for α-$ScH_{0.25}$ and α-$YH_{0.18}$. Ignoring any high-energy contributions from multiphonon scattering, the entire Gaussian-shaped α-$ScH_{0.25}$ spectrum can be fitted just as well with two broad Gaussian components, each ca. 10 meV FWHM in width and separated by 4 meV at positions of 102.8±2 meV. Hence, this suggests that, even if a 4-meV splitting exists for α-ScH_x, it would not necessarily be observable if the component peaks were considerably broadened. In contrast, the visible splitting in the $YH_{0.18}$ spectrum shows the presence of much narrower component peaks. Indeed, attempts to fit the complex-shaped spectrum with two Gaussians required peak widths of ca. 4 meV to reproduce the degree of observed separation in the central por-

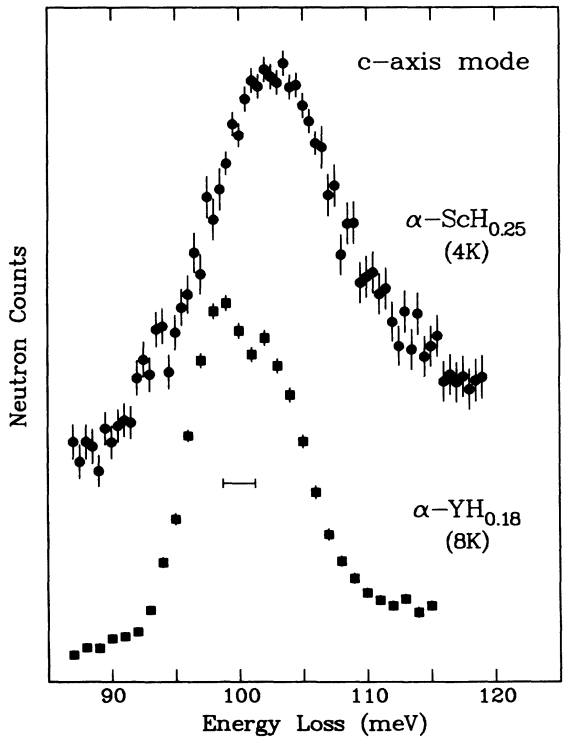

FIG. 5. High-resolution IINS spectra of the c-axis mode at $T < 10$ K for single crystals of α-$ScH_{0.25}$ and α-$YH_{0.18}$.[15] The instrumental resolution (FWHM) is illustrated by the horizontal bar beneath the spectra.

tion of the spectrum, although the mismatched Gaussian peak shapes badly reproduced the observed broadness of the spectral wings.

In short, the overall widths of the α-ScH_x spectra are broader than that of α-$YH_{0.18}$ and are consistent with the presence of H pairing across Sc atoms along the c axis. Moreover, the lack of visible splitting in the α-ScH_x spectra is not inconsistent with this pairing mechanism. Rather, it suggests that the individual components of the c-axis spectra are more broadened than in α-$YH_{0.18}$ due to a larger distribution of H-pair environments (i.e., less extended ordering of H pairs in the c direction) or perhaps a greater variety of intraline and interline arrangements. Thus, it would appear that the hydrogen pairs in α-ScH_x are more disordered than in α-YH_x, which is consistent with the suggestion from the recent NMR studies[13] that the hydrogen arrangements in α-ScH_x are, in some sense, akin to a "proton glass." These conclusions should be contrasted with those based on lower-resolution measurements on α-ScD_x (Ref. 12) where the lack of observable broadening in the c-axis vibration compared to an observed splitting in the vibration peak for α-LuD_x (Ref. 16) led the authors to an optimistic upper limit of 2 meV for a possible splitting of the c-axis mode.

CONCLUSION

An IINS study has been undertaken to characterize the bonding potential of hydrogen in the t sites in α-ScH_x. The potential along the c direction was found to be over 30% softer than in the basal plane and considerably anharmonic as reflected by the deviation of the ratio of second- to first-excited-state energies (1.76) from the harmonic oscillator value. The observed vibrational mode in the basal plane (at ca. 148 meV) was nearly resolution limited, whereas the c-axis mode (at ca. 103 meV) exhibited significant line broadening. High-resolution α-ScH_x spectra of the c-axis mode at low temperature as a function of H concentration failed to resolve any distinct local-mode splitting as was observed previously for α-YH_x. The presence of broadening suggests that hydrogen pairing across Sc atoms along the c axis may be present within α-ScH_x at low temperature. The lack of observable splitting indicates that short-range ordering of the hydrogen pairs in ScH_x is less extensive than in α-YH_x, and suggests a greater variety of intra- and/or interline arrangements.

Previous vibrational spectroscopic measurements of α-$YD_{0.17}H_{0.019}$,[15] in which the H atoms are sufficiently dilute that they can effectively pair only with D atoms across a Y atom, yielded a single narrowed (ca. 6.5 meV) peak at 100 meV instead of the expected doublet at 99 and 103 meV found for H-H pairs in α-$YH_{0.18}$. This observed behavior confirmed that the c-axis mode splitting in α-YH_x is caused by a dynamic coupling mechanism rather than by vibrations in a local potential statically perturbed by pairing. Similar isotope-dilution experiments, utilizing α-$ScD_{0.25}$ doped with a small percentage of H (analogous to the measurements with α-$YD_{0.17}H_{0.019}$), are planned in order to further probe the nature of dynamically coupled hydrogen pairing in this system. Experiments are also underway to study the local c-axis diffusion of hydrogen in the α-ScH_x system.

ACKNOWLEDGMENTS

The authors are indebted to B. J. Beaudry for preparation of the scandium crystals, Professor L. Schlapbach for use of the hydrogen-loading apparatus, U. Meier and J. Hess for help with this apparatus, and N. F. Berk for helpful discussions.

[1]B. J. Beaudry and F. H. Spedding, Metall. Trans. B **6**, 419 (1975).
[2]J. N. Daou, P. Vajda, A. Lucasson, and J. P. Burger, Phys. Status Solidi A **95**, 543 (1986).
[3]J. P. Burger, J. N. Daou, A. Lucasson, P. Lucasson, and P. Vajda, Z. Phys. Chem. Neue Folge **143**, 111 (1985).
[4]R. Danielou, J. N. Daou, E. Ligeon, and P. Vajda, Phys. Status Solidi A **67**, 453 (1981).
[5]C. K. Saw, B. J. Beaudry, and C. Stassis, Phys. Rev. B **27**, 7013 (1983).
[6]D. Khatamian, C. Stassis, and B. J. Beaudry, Phys. Rev. B **23**, 624 (1981).
[7]D. Khatamian, J. Less-Common Metals **129**, 153 (1987).
[8]M. W. McKergow, D. K. Ross, J. E. Bonnet, I. S. Anderson, and O. Schaerpf, J. Phys. C **20**, 1909 (1987).
[9]J. E. Bonnet, D. K. Ross, D. A. Faux, and I. S. Anderson, J. Less-Common Metals **129**, 287 (1987).
[10]O. Blaschko, G. Krexner, J. N. Daou, and P. Vajda, Phys. Rev. Lett. **55**, 2876 (1985).
[11]O. Blaschko, G. Krexner, J. Pleschiutschnig, G. Ernst, J. N. Daou, and P. Vajda, Phys. Rev. B **39**, 5605 (1989).
[12]O. Blaschko, J. Pleschiutschnig, L. Pintschovius, J. P. Burger, J. N. Daou, and P. Vajda, Phys. Rev. B **40**, 907 (1989).
[13]L. R. Lichty, J.-W. Han, R. Ibanez-Meier, D. R. Torgeson, R. G. Barnes, E. F. W. Seymour, and C. A. Sholl, Phys. Rev. B **39**, 2012 (1989).
[14]I. S. Anderson, J. J. Rush, T. Udovic, and J. M. Rowe, Phys. Rev. Lett. **57**, 2822 (1986).
[15]I. S. Anderson, N. F. Berk, J. J. Rush, and T. J. Udovic, Phys. Rev. B **37**, 4358 (1988).
[16]O. Blaschko, G. Krexner, L. Pintschovius, P. Vajda, and J. N. Daou, Phys. Rev. B **38**, 9612 (1988).
[17]S. W. Lovesey, *Theory of Neutron Scattering from Condensed Matter* (Clarendon, Oxford, 1984), Vol. 1.
[18]I. S. Anderson, T. J. Udovic, J. M. Rowe, and J. J. Rush, in *Neutron Scattering Studies of Hydrogen in Yttrium*, edited by F. J. Shorten, Nat. Bur. Stand. (U.S.) Technical Note No. 1217 (U.S. GPO, Washington, D.C., 1985), p. 25.
[19]N. Wakabayashi, S. K. Sinha, and F. H. Spedding, Phys. Rev. B **4**, 2398 (1971).